Proceedings of the 9ICEG
9th International Congress on Environmental Geotechnics
25-28 June, 2023 | Chania, Greece

https://doi.org/10.53243/ICEG2023-194

Effect of different drying techniques on calcium carbonate precipitation using MICP

Renu[1*]; Raja Murugan[2]; Shubham Moudgil[3]; Dali Naidu Arnepalli[4]

[1,3]Research Scholar, Indian Institute of Technology Madras,

Chennai-600036, India. email: [1]renu48838joshi@gmail.com; [3]ishubhammoudgil@gmail.com

[2]Research Scholar, Indian Institute of Technology Madras,

Chennai-600036, India. email:[2]rajabiotech94@gmail.com

*[4]Professor, Indian Institute of Technology Madras, Chennai-600036, India, email: arnepalli@iitm.ac.in; *Corresponding author*

ABSTRACT

The demand for suitable ground for construction has led to the development of various approaches to improve soils with inferior engineering properties. These include conventional techniques like ground compaction, soil reinforcement, lime stabilization, and applying admixtures made of chemical and cementitious compounds. However, some of these methods are cost-intensive and neither economical nor environment-friendly. Given this, MICP (microbially induced calcite precipitation) is emerging as an environmentally friendly technique for soil stabilization. MICP utilizes bacteria to precipitate calcium carbonate for bridging soil pores and helps in soil strengthening. The present study investigates the effect of different drying techniques on MICP. Drying techniques like oven drying and lyophilization have different effects on crystal stabilization. Change in calcium carbonate morphology occurs with time and is related to moisture loss. The drying affects the crystal size, and the temperature affects the moisture loss rate, affecting the total amount of moisture evaporated. SEM images show the changes in crystal size with temperature and rate of drying. XRD analysis was done to assess the effects of different drying techniques on crystal morphology. As the size and morphology of calcium carbonate crystals directly control the strength of the sample in the case of MICP treatment, hence the variation in temperature and rate of drying can be used for effective crystal precipitation in MICP.

Keywords: drying techniques, oven dry, lyophilization, crystal size, crystal morphology

1. INTRODUCTION

Earth contains ample amounts of minerals; however, calcium carbonate ($CaCO_3$) is one of the most frequently used minerals. It has found its application in rubber, plastic, paint, food, and other industries. It is commonly used as a filler in many industrial applications. Excellent biodegradability and biocompatibility have made it a popular low-cost economical material (Chong et al., 2014; Dang et al., 2017). $CaCO_3$ is found to exist in the form of many polymorphs. Three polymorphs of $CaCO_3$ exist, namely calcite, aragonite, and vaterite. Out of all, calcite is the most stable form as it is thermodynamically stable, which makes it very important for industries. However other two polymorphs are vaterite and aragonite, which require either kinetic or biochemical stabilization (Kirboga & Oner, 2013). Many factors affect the precipitation of $CaCO_3$. Control over new crystal nucleation, growth of existing crystals, mixing intensity, seed crystals and solution saturation and pH, etc., are required to obtain the desired crystals (Kirboga & Oner, 2013; Konopacka-Łyskawa et al., 2019). However, all complex synthetic approaches make the task very challenging. There is a need to develop a simple and rapid procedure to synthesize $CaCO_3$.

MICP is emerging as a technique that utilizes ureolytic bacteria to precipitate $CaCO_3$ by urea hydrolysis pathway (Cheng et al., 2014; Lv et al., 2022; Murugan et al., 2021; Phillips et al., 2013). MICP is relatively easy, inexpensive, and environmentally friendly (DeJong et al., 2010). MICP can effectively precipitate $CaCO_3$ and can be used for soil stabilization (Chen et al., 1938; Leon A. van Paassen et al., 2010). These crystals precipitate at the grain contact points and increase the soil strength (Li et al., 2022; Song et al., 2021; Zhao et al., 2022). There are different metabolic pathways involved in MICP; however, urea hydrolysis is the most famous and well-researched (Dhami et al., 2013). In MICP,

ureolytic bacteria secretes urease enzyme via urea hydrolysis and hydrolyses urea for its metabolism. This hydrolyzed urea converts into carbonate and precipitates $CaCO_3$ in the presence of a calcium source.

This paper focuses on the utilization of MICP for $CaCO_3$ synthesis. The synthesized crystals can be used for geomaterial stabilization. Research has shown that MICP has the potential to become an environmentally friendly technique to stabilize soil with inferior engineering characteristics (Lv et al., 2022; Phillips et al., 2013; van Paassen et al., 2009). For this purpose, first, the bacteria is procured and grown. Thereafter the bacterial growth analysis was done. This is followed by the qualitative and quantitative analysis of its urease activity. After the confirmation of the urease activity of bacteria, it was transferred to cementation media and allowed for cementation. In MICP, drying is commonly done for the stabilization of precipitated crystals for full solidification and hardening of the $CaCO_3$ (Dubey et al., 2022; Jain, 2020; Lv et al., 2022). However, the drying method and temperature affect the size and morphology of precipitated crystals (Cheng et al., 2014; Febrida et al., 2020; Siegel & Reams, 1966). Drying mainly affects the size of precipitated crystals, and the moisture loss rate affects the morphology of $CaCO_3$ (Febrida et al., 2020; Sabri et al., 2016; Siegel & Reams, 1966). The temperature of the surroundings determines the rate of moisture loss. Hence the effects of different drying methods on crystal type, size, and morphology in the MICP process are observed. For the above purpose, two methods of drying, namely oven drying and freeze drying, were adopted as they were commonly used in literature and their effect on crystal size and morphology was observed. Scanning electron microscopy was done to ascertain the size and morphological characteristics, followed by XRD for its characterization. FTIR and EDS analysis was done to confirm the presence of $CaCO_3$.

2. MATERIALS AND METHODOLOGY

In the present study, Sporosarcina Pasteurii, an American-type culture (ATCC 11859), is used for microbially induced calcite precipitation (MICP). This microbe was chosen because it was the most commonly used microbe in literature. The bacteria were grown in an (ATCC 1376) media comprised of 20 g/l yeast extract, 10 g/l ammonium sulphate and 0.13 M tris base at pH 9. All the media components were mixed after autoclaving at 121 °C at 15 psi pressure for 20 minutes (Murugan et al., 2021). No growth was observed if ingredients were mixed before autoclaving. All the experiments were performed in a laminar airflow chamber. For the growth of microbial culture, test tubes were left for incubation overnight at 37 °C at 160 rpm in an incubator shaker. After 9 hours, turbidity in the tube confirms the growth of the bacteria.

After subculturing twice, the culture was used for optical density (OD) measurement and cementation solution. For the OD measurement, culture was taken and centrifuged at 8000 rpm for 15 minutes, and the temperature was maintained at 4 °C using temperature controlled centrifuge. The centrifuged pellet was later washed with NaCl. The OD was determined at a wavelength of 600 nm for bacterial density estimation using a UV-visible spectrophotometer.

For the preparation of cementation media, an equimolar filter sterilized $CaCl_2$ and urea of 0.5 M concentration were mixed in 2 g/l of autoclaved yeast extract. Cells grown in ATCC 1376 media were taken and centrifuged. Discarding the supernatant, the cell pellet was mixed in a cementation solution (Murugan et al., 2021). A cementation solution of 0.5 OD cells was taken and kept in a shaker overnight. The precipitated crystals were filtered and kept for oven drying and lyophilization.

2.1 Growth kinetics of *Sporosarcina pasteurii*

For the growth kinetics of bacteria, 1 ml of culture was taken at every 1-hour interval and centrifuged and washed with NaCl twice to remove all the cell debris. The optical density of the culture was taken, keeping NaCl as a blank at 600nm using a UV-visible spectrophotometer. After obtaining the OD value, the variation of OD with time was plotted.

2.2 Qualitative assessment of urease activity of bacteria

Urea agar indicator plates were made to confirm the urease positivity of selected microbes. Urea indicator plates composition was peptone and dextrose of 1 g each, sodium chloride of 5 g, disodium phosphate of 1.2 g, monopotassium phosphate of 0.8 g, phenol red of 0.012 g, agar of 15 g and urea

of 20 g in one litre of deionized sterile water having pH 6.8±0.2 increase in the pH of media from 6.8-8.1 will confirm the production of ammonia and carbon dioxide is due to the hydrolysis of urea by urease-producing bacteria. The Agar plate colour changes from light yellowish orange to pink due to the phenol red indicator, which will confirm the urease positivity of bacteria (Stabnikov et al., 2013).

2.3 Quantitative analysis of urease activity of bacteria

For the quantitative analysis of urease activity, the Nesslerisation assay method was used (ASTMD1426, 2008).100 ml of nutrient broth and urea media were prepared in a flask. Composition of nutrient broth- urea media was maintained as 8 g NB and 20 g urea in 1-litre water. At particular OD, the sample was taken and centrifuged at 20000 rpm at 4°C for 10 minutes. Further, the supernatant was collected for a urease activity test. 1 ml of zinc sulphate solution was added to 100 ml aliquot. Zinc sulphate was made by adding 100 g of zinc sulphate hepahydrate ($ZnSO_4 \cdot 7H_2O$) into the water and further diluted to 1 litre. Further sodium hydroxide was added till the pH reached 10.5. 25 ml of the first filtrate was discarded after filtration. Now *S* ml of filtrate is taken and diluted to 50 ml in Nessler's tube. 2 drops of sodium potassium tartrate solution were added to prevent cloudy tubes. Further, 1 ml of Nessler's reagent was added to the sample. Then wavelength at 425 nm was measured. Further ammonia nitrogen can be calculated corresponding to OD values observed from the standard curve as,

$$\text{Ammonia Nitrogen(E) in ppm} = \frac{A \times 1000}{S} \quad (1)$$

Where, A is ammonia nitrogen observed in mg, and *S* is the sample amount taken in ml.

$$\text{Ammonia (ppm)} = E \times 1.22 \quad (2)$$

One unit of urease activity is defined as the amount of enzyme that catalyzes the hydrolysis of 1-µM urea per minute (Kang et al., 2014).

2.4 Biomineral precipitation

The bacterial solution was taken and centrifuged, discarding the supernatant; the pellet was transferred into 100 ml of cementation solution, making final OD of 0.5. The cementation solution was kept overnight, and the precipitated crystals found were filtered using a vacuum filtration technique. And the supernatant was stored for bi-product ammonia concentration measurement. Precipitated crystals were dried using two different techniques, namely oven drying, and lyophilization.

2.5 Quantification of ammonia

The supernatant of the cementation solution was used for MICP bi-product ammonia quantification after bio-mineral precipitation. The Phenol hypochlorite method was used for the same (Murugan et al., 2022). 200 µL of phenol nitroprusside reagent and 200 µL of alkaline hypochlorite were mixed with 750 µL of 500 times diluted sample. Then the mixture was left for incubation for 30 minutes at a temperature of 37°C. The optical density of the sample was measured at 626 nm and compared with standard plots. The standard of 0-100 µM was prepared in the same manner using ammonium sulphate salt.

2.6 Mineralogical and morphological analysis of precipitated minerals

The precipitated biomineral sample was pulverized for mineralogical analysis using the X-ray diffraction technique and evenly distributed over the glass slide placed on the sample stage. The sample interacted with X-rays using Cu-K_α as source radiation containing 1.54 Å of wavelength, nickel filter, monochromator, and X'celerator detector placed over a goniometer.

For the morphological analysis of precipitated crystals scanning electron microscope (SEM, Philips FEI Quanta 200, USA) was used. The gold sputtering was done for around 60 seconds on crystals glued on carbon tape and gold palladium. The samples were placed in a vacuum chamber, and the sample was scanned by a beam of electrons striking the sample. Surface morphology was characterized by the signal produced by the sample and secondary electrons.

Fourier-transform infrared spectroscopic analysis (FTIR) was used to characterize carbonate bonds in precipitated biomineral, as shown in Figure 5. The sample was mounted over the diamond crystal then IR spectra of 400-4000 cm^{-1} were obtained using attenuated total reflectance (ATR) mode. The compressive load was applied to powder from a micrometre-controlled pressure pin to ensure intimate contact between the sample and biomineral. The noise was removed from obtained absorption spectra, and peak positions corresponding to particular wave numbers were identified.

3. RESULTS AND DISCUSSIONS

3.1 Growth curve of sporosarcina pasteurii

From the growth kinetics study, the following growth curve was obtained for sporosarcina pasteurii, as shown in Figure 1. It can be seen from the growth curve that bacteria take a lag time of around 1 hour to get acquainted with food, and after that, exponential growth was observed. After 5 hrs, the rate of growth slows down, and bacteria finally reaches the stationary phase.

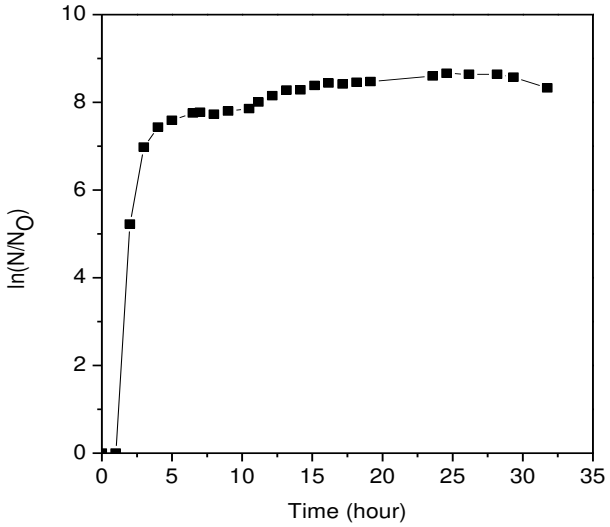

Figure 1. *Growth curve of Sporosarcina Pasteurii*

3.2 Qualitative and quantitative analysis of urease activity and residual ammonium cementation solution

The qualitative analysis of urease activity was confirmed by the change in colour of the urea agar plate to pink, as shown in figure 2. This colour change confirms the ureolytic ability of bacteria (Stabnikov et al., 2013).

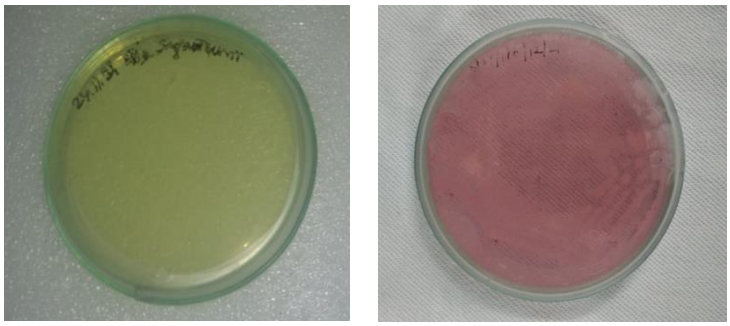

Figure 2. *Change in urea indicator plates from yellowish orange to pink*

Later the quantitative assessment was done for urease activity using the Nesselerization assay method (ASTM D1426, 2014). The optical density of 5 times diluted samples taken at 6.5 hours was observed at 1.6765. And from the standard curve, the equation depicting the relationship between ammonia and optical density (OD) is as below,

$$OD_{425} = 0.1036 \times \text{Ammonia} \quad (3)$$

Ammonia corresponding to an OD of 1.676 was calculated as 13.889 ppm. One unit of urease activity is defined as the amount of enzyme that catalyzes the hydrolysis of 1-μM urea per minute (Kang et al., 2014). As one mole of urea is equivalent to two moles of ammonia, the urease activity of the bacteria was found to be 1045.5 U/ml.

3.3 Quantitative analysis of Ammonia conversion after cementation

For the quantification of ammonia produced after cementation,the phenol hypochlorite method was used. The OD of the collected supernatant at 626 nm after dilution was found to be 0.447. This indicates that ammonia generation is 212.04 mM. As 1 mole of urea gets converted to 2 moles of ammonia, implying out of 500 mM urea, 21.204% got converted to ammonia.

3.4 Mineralogical and morphological characterization of precipitated biominerals by different drying methods

The x-ray diffraction showed that the precipitated sample dried by oven drying and lyophilization was both calcite as shown in figure 3.

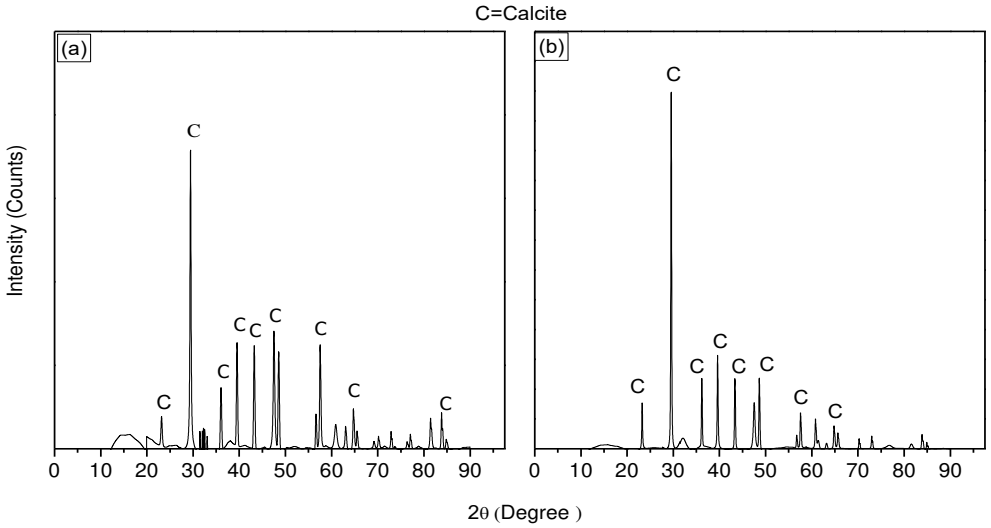

Figure 3. *XRD Spectrum of calcium carbonate crystals precipitated; (a) Oven dried sample, (b) Lyophilized sample.*

The SEM images of precipitated crystals are shown below in figure 4. The crystals were found to be irregular and rhombohedral in shape as calcite. Tubular and elongated needle-type crystals were observed with many pores in the crystals dried via lyophilization; however, plate-like agglomerated crystals were observed in crystals dried using the oven drying method. In lyophilization or freeze drying, first, the product is frozen, and all water gets nucleated to ice. In the later stage, sublimation occurs, which is known as primary drying. The third stage is secondary drying, in which bound water is removed from the structure. Due to the sublimation of ice, porous plugs get formed in the spaces occupied by ice crystals (Degobert & Aydin, 2021). Ice crystals formed due to freezing can grow larger if the rate of freezing is high and the temperature is very low, causing swelling during lyophillization. This swelling can damage the sample, creating very big voids. As the previously frozen product is not allowed to melt, it prevents shrinkage and produces highly porous material, which is different from oven drying, as can be seen from the SEM images shown in figure 4.

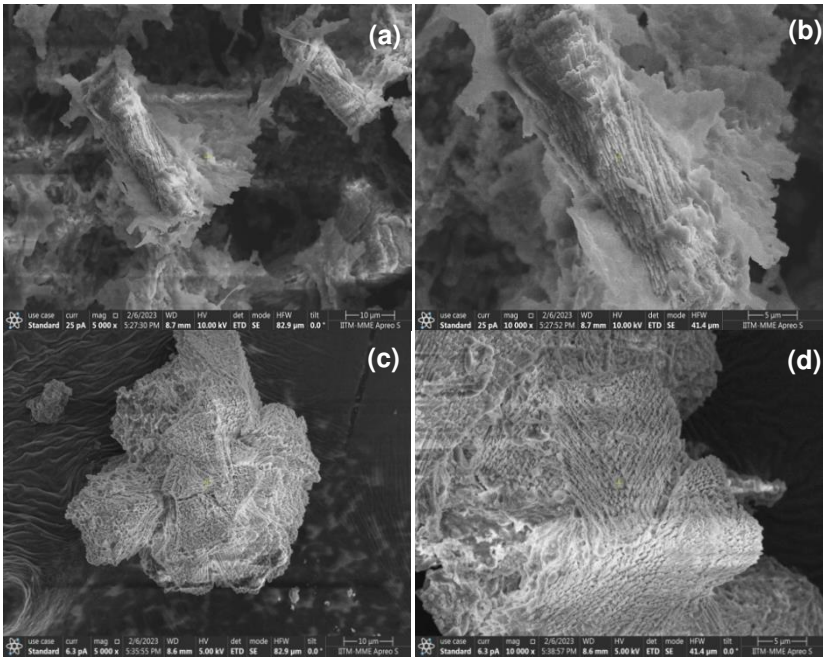

Figure 4. *SEM image at a magnification of 5000x & 10000x, (a) &(b) are lyophilized crystals, (c)&(d) are oven-dried crystals.*

In FTIR it is observed that there exist characteristic shapes and positions of bands for every calcium carbonate polymorph (Padmaraj & Arnepalli, 2022; Wang et al., 2006). The band at 1410 cm^{-1} (asymmetric stretching) and 875 cm^{-1} (out-of-plane bending) suggests the presence of a strong calcite band, as shown in figure 5. There are three oxygen bonded to carbon in the structure of carbonate ion. The stretching motion of these carbon-oxygen bonds because of the interaction with IR rays can result in two types of stretching: symmetric stretching and asymmetric stretching, and bending motion resulting in two types of bending: in-plane bending and out-of-plane bending. In this case, the asymmetric stretching at the 1410 cm^{-1} band results due to the asymmetrical stretching motion of two carbon-bonded oxygens around the bond axis. The out-of-plane bending at 875 cm^{-1} results from the out-of-plane motion of oxygen atoms from the rest of the carbonate groups. The presence of both the bands in lyophilized and oven-dried samples suggests that both the precipitated crystals were calcite, as confirmed by XRD analysis. However, the crystal structure of lyophilized sample is porous in structure, as shown in SEM images.

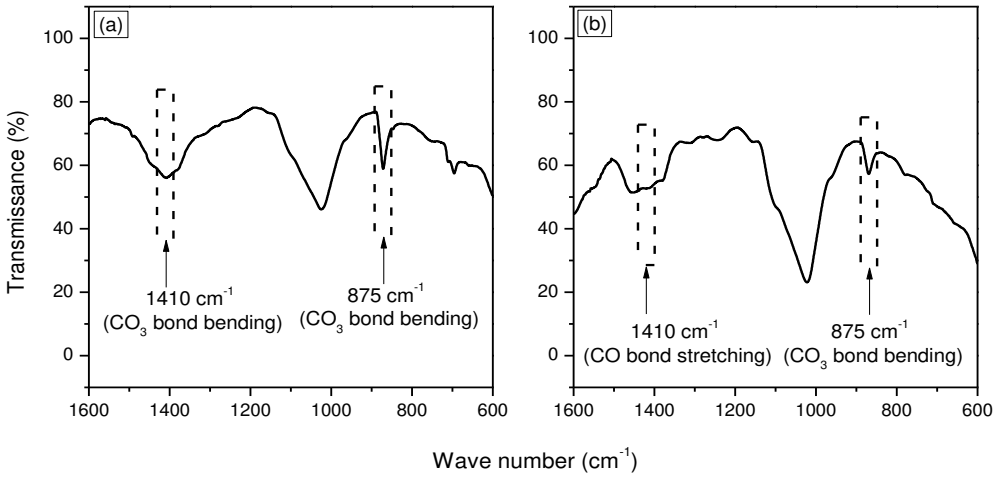

Figure 5. *FTIR analysis of bio mineral formed; (a) Oven dried sample, (b) Lyophilized sample*

4. CONCLUSIONS

The objective of the current study was to synthesize $CaCO_3$ by the use of bacteria and the effect of different drying techniques on the precipitated biomineral. The ureolytic activity of bacteria sporosarcina pasteurii was confirmed by both qualitative and quantitative analysis. After confirmation, the bacteria was used in a cementation solution consisting of urea and $CaCl_2$, which effectively precipitated biomineral calcium carbonate. The ammonia present in the supernatant after crystal precipitation confirms the conversion of urea to carbonates. It was observed from XRD analysis that precipitated biomineral were calcite; however, different drying techniques affected their shape and morphology, as shown in SEM images. SEM images show that the crystals dried using lyophilization were more porous and had an elongated tubular needle-type shape. However, the crystals precipitated via oven drying were agglomerated and deposited in plate-like structures. The FTIR spectra also confirm the presence of calcite bonds in the biomineral. These results show that MICP can effectively be used for $CaCO_3$ precipitation, and the morphology of the crystal can be varied by employing different drying methods.

The findings from the study highlight the calcium carbonate precipitation ability of sporoasarcina pasteurii via ureolysis pathway in MICP and the effects of different drying techniques on crystal stabilization. This study discusses the critical role of various drying techniques in stabilizing precipitated calcium carbonate crystals. It helps improve understanding of the fundamental governing mechanisms and contributes towards future MICP application optimization.

This method proves that the abundance of bacteria in soil can be advantageous as they can be utilized for soil stabilization. This bacteria can be used to improve the strength of soil by binding the soil pores with calcium carbonate. This would be helpful in the field-scale implementation of in-situ soil for MICP applications.

5. FUTURE SCOPE

This study covered the ability of the MICP process to produce a cementitious compound, i.e., $CaCO_3$. Despite being a new interdisciplinary technology, it has good environmental adaptability and has the potential to become a new bio-geotechnical method for soil strength enhancement. This method can pave the way for future geotechnical applications. However, the field implementation of MICP still has some limitations. Mitigations of these limitations require further research and innovations.

a. More studies can be done with different temperature ranges of drying. Modelling this phenomenon will help optimize the method for future field scale implementation.

b. As chemicals used in MICP are expensive, more study is needed to find economic alternatives. This requires a proper cost-benefit analysis with different options.

c. The use of native bacteria or bio-stimulation will be beneficial as an adaptation of foreign bacteria faces difficulties due to harsh environmental conditions and competition with the existing bacteria when used in the field.

d. Bi-product of MICP is ammonia which is harmful to the environment and hence requires proper treatment before disposal.

e. Work in this area requires the collaboration and expertise of biotechnical and geotechnical professionals. More insight into the process will broaden the application of MICP.

REFERENCES

ASTM Standard D1426. (2008). Standard Test Methods for Ammonia Nitrogen In Water. ASTM International, September, 1–7. https://doi.org/10.1520/D1426-08.

Chen, Y.-Q., Wang, S.-Q., Tong, X.-Y., & Kang, X. (1938). Crystal transformation and self-assembly theory of microbially induced calcium carbonate precipitation. Applied Microbiology and Biotechnology, 1, 3. https://doi.org/10.1007/s00253-022-11938-7

Cheng, L., Shahin, M. A., Cord-Ruwisch, R., Addis, M., Haranto, T., & Elms, C. (2014). Soil stabilisation by microbial induced calcium carbonate precipitation: investigation of some important physical and environmental aspects. In: 7th International Congress on Environmental Geotechnics, 10 - 14 November, Melbourne, Australia, November, 10–14.

Chong, K. Y., Chia, C. H., Zakaria, S., & Sajab, M. S. (2014). Vaterite calcium carbonate for the adsorption of Congo red from aqueous solutions. Journal of Environmental Chemical Engineering, 2(4), 2156–2161. https://doi.org/10.1016/j.jece.2014.09.017

Dang, H. C., Yuan, X., Xiao, Q., Xiao, W. X., Luo, Y. K., Wang, X. L., Song, F., & Wang, Y. Z. (2017). Facile batch synthesis of porous vaterite microspheres for high efficient and fast removal of toxic heavy metal ions. Journal of Environmental Chemical Engineering, 5(5), 4505–4515. https://doi.org/10.1016/j.jece.2017.08.029

Degobert, G., & Aydin, D. (2021). Lyophilization of nanocapsules: Instability sources, formulation and process parameters. Pharmaceutics, 13(8). https://doi.org/10.3390/pharmaceutics13081112

DeJong, J. T., Mortensen, B. M., Martinez, B. C., & Nelson, D. C. (2010). Bio-mediated soil improvement. Ecological Engineering, 36(2), 197–210. https://doi.org/10.1016/j.ecoleng.2008.12.029

Dhami, N. K., Reddy, M. S., & Mukherjee, M. S. (2013). Biomineralization of calcium carbonates and their engineered applications: A review. Frontiers in Microbiology, 4(OCT), 1–13. https://doi.org/10.3389/fmicb.2013.00314

Dubey, A. A., Murugan, R., Ravi, K., Mukherjee, A., & Dhami, N. K. (2022). Investigation on the Impact of Cementation Media Concentration on Properties of Biocement under Stimulation and Augmentation Approaches. Journal of Hazardous, Toxic, and Radioactive Waste, 26(1), 1–13. https://doi.org/10.1061/(asce)hz.2153-5515.0000662

Febrida, R., Herda, E., Cahyanto, A., & Made Joni, I. (2020). Effect of drying technique on the synthesis of calcium carbonate by simple solution method. AIP Conference Proceedings, 2219(May). https://doi.org/10.1063/5.0003073

Jain, S. (2020). Stabilization of coarse-grained geomaterial by biochemical process Doctor of Philosophy Department of Civil Engineering Indian Institute of Technology Madras Chennai-600036.

Kang, C. H., Choi, J. H., Noh, J. G., Kwak, D. Y., Han, S. H., & So, J. S. (2014). Microbially Induced Calcite Precipitation-based Sequestration of Strontium by Sporosarcina pasteurii WJ-2. Applied Biochemistry and Biotechnology, 174(7), 2482–2491. https://doi.org/10.1007/s12010-014-1196-4

Kirboga, S., & Oner, M. (2013). Effect of the experimental parameters on calcium carbonate precipitation. Chemical Engineering Transactions, 32, 2119–2124. https://doi.org/10.3303/CET1332354

Konopacka-Łyskawa, D., Czaplicka, N., Kościelska, B., Łapiński, M., & Gębicki, J. (2019). Influence of selected saccharides on the precipitation of calcium-vaterite mixtures by the CO 2 bubbling method. Crystals, 9(2). https://doi.org/10.3390/cryst9020117

Li, Z., Chen, J., Zhao, G., Xiang, H., & Liu, K. (2022). Effect and mechanism of microbial solid-free drilling fluid for borehole wall enhancement. Journal of Petroleum Science and Engineering, 208(PD), 109705. https://doi.org/10.1016/j.petrol.2021.109705

Lv, C., Tang, C., Zhu, C., Li, W., Chen, T., Zhao, L., & Pan, X. (2022). Environmental Dependence of Microbially Induced Calcium Carbonate Crystal Precipitations : Experimental Evidence and Insights. 148(7), 1–16. https://doi.org/10.1061/(ASCE)GT.1943-5606.0002827

Murugan, R., Sundararaghavan, A., Dhami, N. K., Mukherjee, A., & Suraishkumar, G. K. (2022). Importance of carbon to nitrogen ratio in microbial cement production: Insights through experiments and genome-scale metabolic modelling. Biochemical Engineering Journal, 186(August), 108573. https://doi.org/10.1016/j.bej.2022.108573

Murugan, R., Suraishkumar, G. K., Mukherjee, A., & Dhami, N. K. (2021). Insights into the influence of cell concentration in design and development of microbially induced calcium carbonate precipitation (MICP) process. PLoS ONE, 16(7 July), 1–19. https://doi.org/10.1371/journal.pone.0254536

Padmaraj, D., & Arnepalli, D. N. (2022). Investigations on Carbonation of Lime Stabilized Expansive Soil from Micro-Level Perspectives. 110–119. https://doi.org/10.1061/9780784484012.011

Phillips, A. J., Gerlach, R., Lauchnor, E., Mitchell, A. C., Cunningham, A. B., & Spangler, L. (2013). Engineered applications of ureolytic biomineralization: A review. Biofouling, 29(6), 715–733. https://doi.org/10.1080/08927014.2013.796550

Sabri, I. N., Alias, N., Ali, A. M., & Shaikh Mohammed, J. (2016). Characterization of CaCO3 MICROSPHERES fabricated using distilled water. Malaysian Journal of Analytical Science, 20(2), 423–435. https://doi.org/10.17576/mjas-2016-2002-27

Siegel, F. R., & Reams, M. W. (1966). Temperature Effect on Precipitation of Calcium Carbonate From Calcium Bicarbonate Solutions and Its Application To Cavern Environments. Sedimentology, 7(3), 241–248. https://doi.org/10.1111/j.1365-3091.1966.tb01597.x

Song, C., Elsworth, D., Zhi, S., & Wang, C. (2021). The influence of particle morphology on microbially induced CaCO3 clogging in granular media. Marine Georesources and Geotechnology, 39(1), 74–81. https://doi.org/10.1080/1064119X.2019.1677828

Stabnikov, V., Jian, C., Ivanov, V., & Li, Y. (2013). Halotolerant, alkaliphilic urease-producing bacteria from different climate zones and their application for biocementation of sand. World Journal of Microbiology and Biotechnology, 29(8), 1453–1460. https://doi.org/10.1007/s11274-013-1309-1

van Paassen, L. A., Harkes, M. P., Van Zwieten, G. A., Van Der Zon, W. H., Van Der Star, W. R. L., & Van Loosdrecht, M. C. M. (2009). Scale up of BioGrout: A biological ground reinforcement method. Proceedings of the 17th International Conference on Soil Mechanics and Geotechnical Engineering: The Academia and Practice of Geotechnical Engineering, 3, 2328–2333. https://doi.org/10.3233/978-1-60750-031-5-2328

van Paassen, Leon A., Ghose, R., van der Linden, T. J. M., van der Star, W. R. L., & van Loosdrecht, M. C. M. (2010). Quantifying Biomediated Ground Improvement by Ureolysis: Large-Scale Biogrout Experiment. Journal of Geotechnical and Geoenvironmental Engineering, 136(12), 1721–1728. https://doi.org/10.1061/(asce)gt.1943-5606.0000382

Wang, C., Zhao, J., Zhao, X., Bala, H., & Wang, Z. (2006). Synthesis of nanosized calcium carbonate (aragonite) via a polyacrylamide inducing process. Powder Technology, 163(3), 134–138. https://doi.org/10.1016/j.powtec.2005.12.019

Zhao, Y., Wang, Q., Yuan, M., Chen, X., Xiao, Z., Hao, X., Zhang, J., & Tang, Q. (2022). The Effect of MICP on Physical and Mechanical Properties of Silt with Different Fine Particle Content and Pore Ratio. Applied Sciences (Switzerland). https://doi.org/10.3390/app12010139